Calculation for fission decay from heavy ion reactions at intermediate energies

Th. Blaich,* M. Begemann-Blaich,† M. M. Fowler, and J. B. Wilhelmy
Los Alamos National Laboratory, Los Alamos, New Mexico 87545

H. C. Britt, D. J. Fields, L. F. Hansen, M. N. Namboodiri, and T. C. Sangster
Lawrence Livermore National Laboratory, Livermore, California 94550

Z. Fraenkel
Weizmann Institute of Science, 76100 Rehovot, Israel
(Received 19 June 1991)

A detailed deexcitation calculation is presented for target residues resulting from intermediate-energy heavy ion reactions. The model involves an intranuclear cascade, subsequent fast nucleon emission, and final decay by statistical evaporation including fission. Results are compared to data from bombardments with Fe and Nb projectiles on targets of Ta, Au, and Th at 100 MeV/nucleon. The majority of observable features are reproduced with this simple approach, making obvious the need for involving new physical phenomena associated with multifragmentation or other collective dissipation mechanisms.

PACS number(s): 25.70.Jj, 25.70.−z, 25.85.−w

I. INTRODUCTION

The fission of a heavy nuclear system provides an excellent tool for studying the latter stages of a complex, high-energy nuclear reaction. Coulomb energy systematics give a clear indication for the binary fission process while fragment angular correlations and mass and energy distributions can be used to estimate average quantities such as linear momentum transfer and mean mass and excitation energy of the fissioning system. A comprehensive review of fission utilized as a filter for studying reaction mechanisms has recently been published by Viola [1].

Since fission is a slow process which occurs from an equilibrated nuclear system, it is particularly valuable for studies of the target residues remaining after a high energy nuclear collision. In the mass 150–250 region fission is particularly useful because of the detailed information available on the fission barriers as a function of excitation energy and angular momentum [2,3]. This knowledge allows a reliable calculation of fission probabilities in the second stage of a two-step nuclear reaction, if the first step of the reaction can be described well enough to yield distributions of the residues as a function of charge, mass, excitation energy, and angular momentum. Conversely, a comparison of the fission predictions from a comprehensive model with experimental data can be used to test in an integral manner the predictions for the residue distributions from the early stage of the reactions and possibly to search for new phenomena. In particular, sensitive tests of such a model can be obtained by investigating the subsequent fission decay as a function of mass loss and linear momentum of the surviving residual products.

This two-step picture clearly assumes that fission is a slow process which samples the target residues only after they have lost a large fraction of their excitation energy. There is evidence from compound nucleus studies as well as medium-energy heavy ion reactions that this assumption is valid [4]. The fissility is also sensitive to Z^2/A, and, therefore, additional insight is obtained by comparing different target-projectile combinations which produce nuclei with similar excitation energy and spin, but different values of Z^2/A. This makes fission an ideal probe to test reaction models that deal with the deexcitation of the residues.

In heavy ion reactions at energies of 100 MeV/nucleon and above, intranuclear cascade models (INC) [5,6] have been successful in predicting the properties of the prompt emission associated with the initial direct cascade. However, there have been few tests of the accuracy to which they can predict the detailed properties of the target residues left over after the fast cascade, since little has been done to model or measure in detail the decay of these highly excited residues. In principle, these residues can be treated in a manner similar to the compound systems produced in heavy ion reactions at much lower energies. This approach is particularly attractive in cases where the residue undergoes fission since this decay channel comes unambiguously from an equilibrated residue at a late time.

From the systematics of momentum transfer to fissioning residues in high-energy heavy ion collisions there is strong evidence that fission is predominantly associated with peripheral collisions and that the maximum excitation energies for residues associated with fission decay are limited to a few hundred MeV [7,8]. The origin of this limiting behavior is believed to arise because the residues following a more central collision are too light to have a significant fission branch. However, these results cannot distinguish whether this is due to the onset of a new process such as multifragmentation or whether it is simply that the fast nucleon cascade leads to residue products which are too light to fission. In order to try to differentiate these two possibilities it is interesting to test the data against a quantitative model of the reaction which contains our best knowledge of the fast cascade

*Present address: UNI Mainz, D-6500 Mainz, Germany.
†Present address: GSI, D-6100 Darmstadt, Germany.

and the fission process. In such a test deviations could give evidence that the fission branch is terminated by the onset of multifragmentation.

In this paper, we present the first attempt to model an entire high-energy heavy ion fission reaction using a two-stage INC/statistical decay approach where the parameters are known to quantitatively fit the particle spectra from the direct stage and from the statistical compound reactions in the residue decay stage. Results are compared to experimental data presented in a companion paper [7] for reactions of 100 MeV/nucleon Fe and Nb projectiles on targets of Ta, Au, and Th. Our analysis uses the Yariv-Fraenkel code [5,6] followed by a preequilibrium fast cascade which leads into a statistical decay mode treated by the code PACE [9]. The primary objective of this paper is to determine if traditional analyses can be applied to fission decay induced in medium-energy heavy ion reactions. We believe that before invoking new physical phenomena involving multifragmentation or other collective dissipation models, it should be established that there are significant systematic deviations that are incompatible with existing models.

II. EXPERIMENTAL DATA

We have performed several experiments to study light particle and intermediate mass fragment (IMF) emission and fission decay using 50 to 100 MeV/nucleon Fe and Nb beams on Ta, Au, and Th targets. The experiments were conducted at the Lawrence Berkeley Laboratory Bevalac low-energy beam line using the PAGODA detector facility [10]. This array of detectors combines excellent charge, velocity, and position resolution for fission-mass fragments with a large dynamic energy range and solid angle coverage. Details of the fission analysis from these experiments are provided in Ref. [7]; only a few salient features will be necessary for the present discussion.

Figure 1 shows a Z_1-Z_2 contour distribution for binary events. The data clearly separate into two distinct regions. The region closest to the origin contains events in which one of the two fragments may be in the fission-mass range but where the sum Z_1+Z_2 is generally less

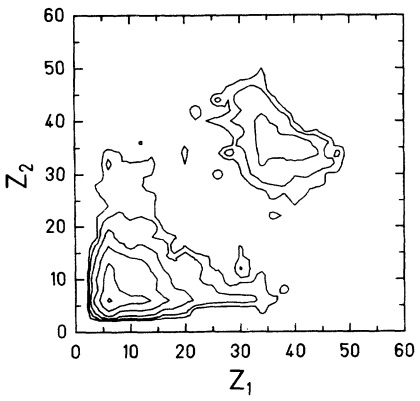

FIG. 1. Correlation of Z_1 vs Z_2 for binary coincidences for which both fragments were fully identified in the PAGODA. The lowest cut is six events per Z bin, the contour lines indicate increases by factors of 2.

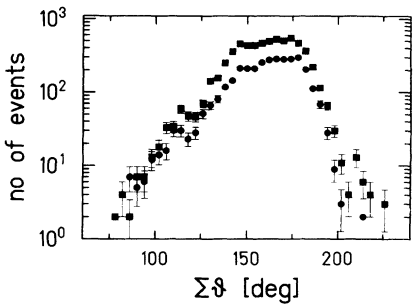

FIG. 2. Folding angle distributions between two fully identified fission fragments (circles) and between one fully identified fragment and a fragment for which only the velocity vector is known (squares). The error bars denote statistical errors.

than half Z_{targ}. This implies that the breakup of the residual system is not binary and that other fragments have been emitted outside the acceptance of the detector array. The other region consists entirely of events in which the sum Z_1+Z_2 is close to but less than Z_{targ} and each fragment has a charge greater than about 25. Besides exhibiting a symmetric binary charge distribution, fragments in this region demonstrate three other characteristics associated with the fission process: (1) they have a narrow phi distribution; (2) the distribution of relative velocities exhibits a narrow peak at the Viola velocity [11]; and (3) the two fragments are observed on opposite sides of the beam. The events in this second region are clearly fission of the target residue. Missing from Fig. 1, however, are those events in which one of the fission-mass fragments is not fully charge identified.

As indicated by Begemann-Blaich *et al.* [7] the PAGODA array does not provide charge identification for fission-mass fragments having velocities less than 1 cm/ns. However, we can assign these slower fragments to fission decay if they are in coincidence with a fully identified fission-mass fragment on the other side of the beam because the distribution of relative velocities peaks sharply at the Viola value. Figure 2 shows the folding angle distributions for binary fission events in which both fragments are completely identified ($v_1, v_2 > 1$ cm/ns) and in which one of the fragments has a velocity less than 1 cm/ns. Since there are no discernable differences between the shapes of these distributions, we also include these slower fragments in our overall fission analysis and model comparisons.

III. FISSION MODELING

For this paper we have chosen to analyze the fission distribution using established intranuclear cascade and statistical deexcitation procedures. In making this choice, our objective is not to arbitrarily adjust model parameters to optimize the fit to the data but to investigate the general applicability of this approach for intermediate-energy reactions. Before more exotic physics such as limiting temperatures or reaction dynamical effects are utilized, we feel it is necessary to establish systematic deviations from the traditional analysis. Therefore, we have chosen the intranuclear cascade model of

Yariv and Fraenkel [5,6] and the statistical deexcitation code PACE [9] utilizing angular momentum dependent fission barriers from Sierk [3]. Though these models are well established, there are several parameters which must be fixed and operational applicability limits must be considered. We have attempted to make reasonable, well-defined choices for the parameters and, where possible, tie these to existing experimental data.

A. Cascade applicability

The intranuclear cascade approach consists of following individual nucleon-nucleon interactions using on-shell scattering amplitudes. This approach does not carry information on any collective aspect of nuclear matter. The model was designed, and clearly is most relevant, for higher energy interactions. Therefore, this analysis has been performed only for the highest beam energies (100 MeV/nucleon) from the PAGODA measurements. Examples of the properties calculated by the intranuclear cascade model are presented in Fig. 3 for the Nb+Au reaction at 100 MeV/nucleon. As a function of the reaction impact parameter, this figure shows four characteristics of the targetlike remnant: (1) the residual excitation energy, (2) primary parallel momentum, (3) nuclear spin, and (4) primary mass number. We see that the correlation between impact parameter and parallel momentum is monotonic and thus we can use parallel momentum as an estimate for impact parameter. In Fig. 4, we present the calculated correlation between the parallel momentum and the residual excitation energy. Within the model calculation this is linear over a wide range of parallel momenta and can thus be used to estimate residue excitation energies for our data.

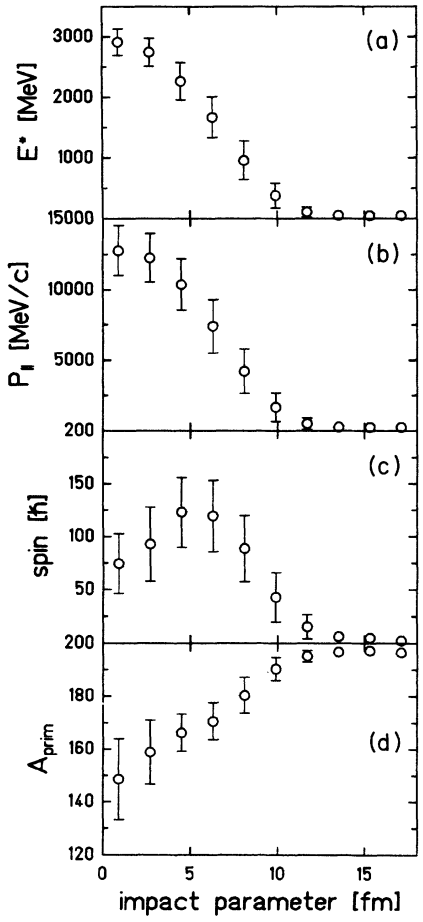

FIG. 3. Results of the intranuclear cascade for Nb+Au at 100 MeV/nucleon. The four parts show (a) excitation energy, (b) parallel momentum, (c) angular momentum, and (d) mass number of the target residues in ten bins of impact parameter. The error bars indicate the widths of the distributions in the respective bins.

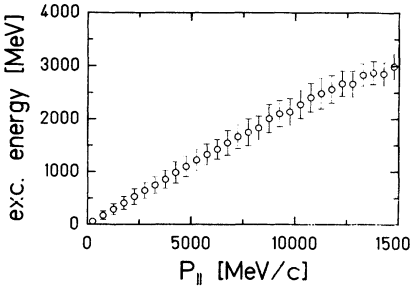

FIG. 4. Correlation between excitation energy and parallel momentum transfer for Nb+Au at 100 MeV/nucleon, as predicted by the intranuclear cascade. The error bars indicate the widths of the distributions in the respective bins.

B. Excitation energy

For target residues with excitations above 1 GeV our estimates show that following the fast cascade (following section) the residual mass is too small to yield a significant fission branch. Furthermore, when the predicted excitation energies approach or exceed the total binding of the nuclear fragment, the INC estimates become unreliable. Therefore we chose to limit our calculations to the region of excitation energies below 1 GeV.

C. High-energy deexcitation

For nuclei produced in the intranuclear cascade calculation having excitation energies between 300 and 1000 MeV, we have introduced a fast nucleon cascade before using a statistical decay analysis. We chose 300 MeV for the transition energy from the fast cascade to statistical analysis because at this energy the neutron decay life time becomes comparable to the transit time of a nucleon with Fermi energy. If the life time is shorter than this, the system cannot be viewed as sequentially emitting particles statistically from a fully equilibrated system, and, therefore, statistical calculations such as PACE are invalid. Also parametrizations of level densities, yrast lines, etc., are based on data from significantly lower energies and cannot be assumed to yield accurate predictions when extrapolated far beyond the range of the data. Though the choice of 300 MeV is fairly arbitrary, we have computationally verified that the exact value of this transition energy is not critical.

For modeling the deexcitation in the 300 to 1000 MeV region we employ a fast nucleon emission mechanism. In

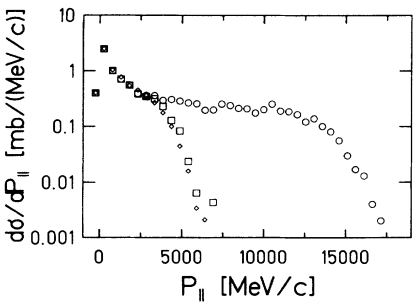

FIG. 5. Parallel momentum transfer distributions for Nb+Au at 100 MeV/nucleon at various stages of the simulation: integral distributions out of INC (circles), distribution truncated by selecting nuclei with $E_x < 1000$ MeV (squares), and distribution after the fast cascade (diamonds).

this decay the choice between proton or neutron emission is based on the relative number of neutrons and protons in the excited nucleus. The particle energy spectrum is taken as a Maxwellian with a slope parameter of 15 MeV. The choice of this parameter is based on a systematic study of particle emission spectra obtained for reactions in this energy regime [12]. The angular momentum removed by these particles is assumed to be $\frac{2}{3}$ of the maximum allowed value (i.e., that associated with tangential emission from the nuclear surface). The factor of $\frac{2}{3}$ arises from geometric weighting of the impact parameters of emission. The cascade particles are assumed to be emitted isotropically in the center-of mass frame of the target residue.

The effect of these choices is shown in Figs. 5 and 6. The original intranuclear cascade analysis produces targetlike residues with parallel momenta up to ≈ 17 GeV/c for the Nb+Au reaction at 100 MeV/nucleon. Since there is essentially a linear dependence between excitation energy and parallel momentum transfer, selecting events having residual excitation energy of $E_x \lesssim 1000$ MeV limits the maximum parallel momentum to ~ 7 GeV/c (Fig. 5).

Figure 6 shows the effect of the excitation energy cutoff and the fast particle emission on the nuclear spin distribution. Both effects reduce the amount of angular momentum in the targetlike residue. From Fig. 6 it is obvious that the cascade produces angular momentum distributions quite different from those obtained in lower-energy heavy ion reactions. The low-energy heavy ion reactions have triangular-shaped angular momentum distributions which have maximum yields for the highest l values. In these cases fission occurs predominantly from the highest l values where the fission barriers are minimum or zero. However, in our case the cascade analysis produces exponential distributions which peak at the lowest l value, much like those obtained in light particle bombardments (e.g., proton or alpha). As a result the cascade-produced nuclei—at least reasonably fissile ones—have a fission decay mode which is more sensitive to excitation energy than angular momentum.

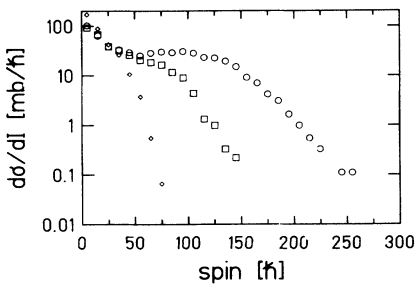

FIG. 6. Spin distributions for Nb+Au at 100 MeV/nucleon at various stages of the simulations. The meaning of the symbols is the same as in Fig. 5.

D. Statistical decay

The original products having $E_x < 300$ MeV and those that were deexcited down to this level by the fast-particle emission process were analyzed using the PACE statistical model code. This code is described elsewhere [9] and we will only list some of its relevant features. The particle emission probabilities are obtained using optical model transition probabilities [13,14] and modified Fermi gas level densities [15]. The version we have used has been modified to include angular momentum dependent fission barriers [3]. We have also modified the code to enable us to follow the deexcitation of any resultant fission products. The fission product mass distribution is assumed to be a Gaussian, centered around symmetric division and having a width calculated from the temperature of the fissioning nucleus with standard statistical formulae [16]. The fission fragments share the excitation energy of the fissioning system proportional to their mass (equal temperature in the two fragments) and are assigned angular momenta based on the sticking limit (which gives comparable values to those obtained from fragment bending mode analyses [17]. The deexcitation of these fission fragments is then followed using the PACE code until they become stable against further particle decay. With these combined procedures we are able to predict final product yield and angular distributions that can be compared directly with the experimental data.

From 300 to 150 MeV of excitation energy the system is allowed to statistically evaporate particles, and the angular momentum is explicitly followed. In this excitation energy range fission is not allowed to compete as a decay channel. This choice is made as a simple approximation for the dissipative and flow dynamic effects that impose minimum times for fission to become a viable decay channel [4,18]. At excitation energies below 150 MeV, fission is allowed as a decay channel in PACE with the relative level density parameters chosen to given $a_f/a_n = 1.01$. The value of a_f/a_n and the cutoff energy for fission were adjusted to give the best representation of previous high-energy proton and light heavy ion data [19,20] as shown in Fig. 7. Changes in the values of these parameters tend to proportionally scale all of the calculated cross sections. Thus, our model has effectively two adjustable parameters that were determined by a fit to the data in Fig. 7 and then held fixed for all subsequent calculations. The same parameters also reproduce, to within 30%, the integral fission cross sections that were measured for erbium and osmium isotopes excited in heavy ion compound-nucleus reactions [2].

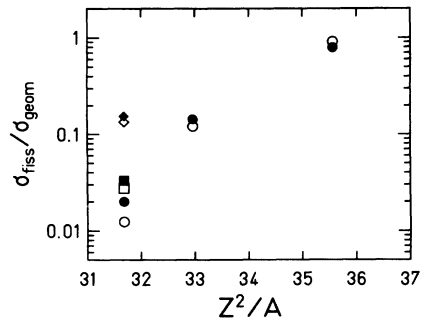

FIG. 7. Comparison between experimental (solid symbols) and calculated (open symbols) fission cross sections. The experimental data are taken from Refs. [21] and [22]. The theoretical values were calculated with the combination of INC and PACE described in this work. The ratios of fission to geometrical cross sections are plotted vs Z_2/A of the target nucleus for protons + Au, Bi, and U at 190 MeV (circles), protons + Au at 600 MeV (squares), and ^{12}C + Au at 84 MeV/nucleon (diamonds). Estimated errors of the experimental data are indicated by the size of the symbols.

IV. COMPARISONS WITH EXPERIMENT

The parameter choices described above have been used to calculate the fission yield observables in the 100 MeV/nucleon data. The number of events calculated in various categories is given in Table I.

The approach we have used is to apply an acceptance filter that includes the experimental geometries and efficiencies to the calculated quantities. The filtered calculations can then be directly compared with the experimental observables. Extensive Monte Carlo simulations were performed in order to find out which quantities have the strongest influence on the acceptance. Our simulations showed that only the parallel momentum and the scattering angle of the fissioning nucleus affect the acceptance. The angular distribution of the fission fragments in the system of the fissioning nucleus does not play a significant role. In our experiments, we can identify the charge, energy, and angles of both fission fragments and from these quantities we compute the fragment momentum vectors on the assumption that the secondary nuclei we observe in our detectors are in the valley of stability. This established a pointing angle for the heavy recoil. Figure 8 shows the experimental and calculated results of this pointing angle as a function of the parallel momentum of the fissioning nucleus for the four 100 MeV/nucleon cases studied (Nb+Au, Fe+Ta, Au, Th). The agreement is excellent and provides confidence for our efficiency filter. The comparison of pointing angles

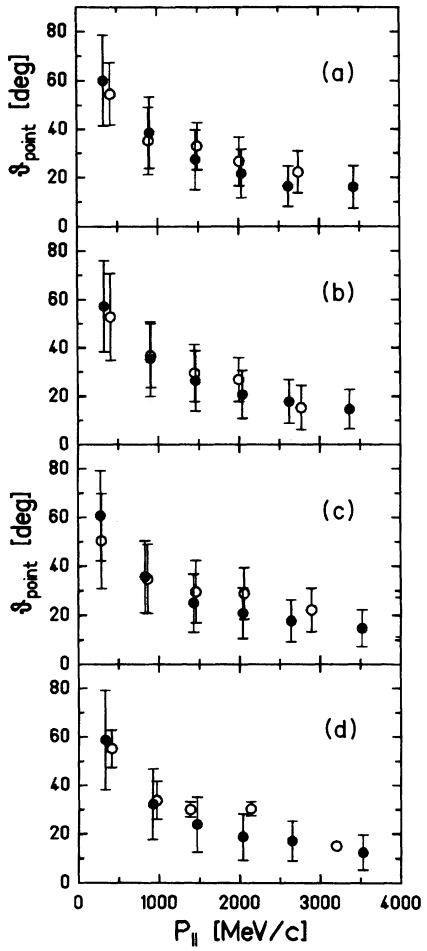

FIG. 8. Comparison between experimental (solid circles) and calculated (open circles) pointing angles as a function of parallel momentum for four target-projectile combinations at 100 MeV/nucleon: (a) Nb+Au, (b) Fe+Au, (c) Fe+Th, and (d) Fe+Ta. The error bars show the widths for the distributions in the respective bins of parallel momentum transfer.

represents the most sensitive test of our acceptance estimates for the experimental apparatus.

Figure 9 presents the calculated and experimental differential cross sections as a function of parallel momentum for the four cases studied. Very good agreement is obtained for three of the four cases. For the Fe+Ta case the experimental results are systematically above the calculated values. The differential shape is in reasonable agreement with the data but the yield is about five times larger than the model prediction. This is the least fissile target and the most sensitive to assumptions regarding angular momentum. However, the pointing

TABLE I. Number of events calculated with INC and used within PACE. A single INC residue has been used several times in PACE in order to increase statistical accuracy for this part of the calculation.

System	Total INC events	INC events $E_x < 1000$ MeV	Total PACE events	Total fission events
Nb+Au	5000	3108	15540	1105
Fe+Au	10000	7137	14274	1032
Fe+Th	3373	2292	9168	6362
Fe+Ta	6591	4822	26732	285

TABLE II. Mean momenta and mean excitation energies from the experimental parallel momentum distributions of Fig. 9. The excitation energies were extracted by means of the theoretical correlation between momentum and energy given in Fig. 4.

System	Mean p_{par} (MeV/c)	Mean E_x (MeV)
Nb+Au	1450	327
Fe+Au	1520	343
Fe+Th	960	217
Fe+Ta	1710	386

angle determination (Fig. 8) indicates no systematic deviation of the acceptance for this reaction.

From the parallel momentum distributions we can infer mean excitation energies of the fissioning nuclei using the correlation between momentum and excitation energy in Fig. 4. The results are given in Table II. The low excitation energies clearly show that fission is a peripheral process for both the Au and Th targets. The excitation can be accounted for by absorption of only two to four nucleons on the average. Within the framework of our calculation, fission diminishes as a viable decay channel at high-energy deposits because the primary nuclei decay by fast-particle emission into nuclei that are too light to fission. This is consistent with the data of Ref. [7] where it is shown that for different projectiles at different energies, fission occurs at the same excitation energy interval.

Figure 10 shows the calculated and observed fission laboratory angular distributions. In the Au case, the peripheral nature of fission is corroborated by the almost complete independence of the fission cross section on the projectile. The cross sections for both Fe and Nb are very similar, which implies that fission comes from reactions which occur at the surface of the nuclei and does not involve a large overlap of target and projectile. These findings substantiate the results of earlier comparisons between intranuclear cascade calculations and fission data [8,21]. As with the momentum transfer distributions, the agreement with the calculation is excellent for the heavier targets. In the case of Ta, the discrepancy in

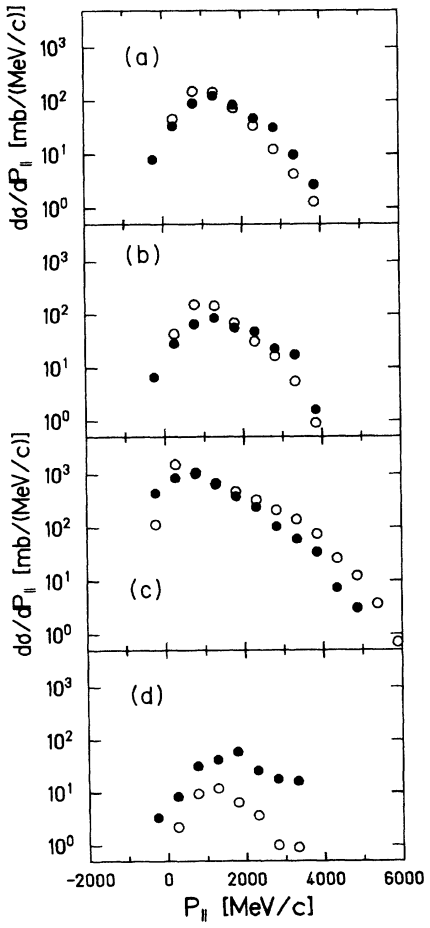

FIG. 9. Comparison between experimental (solid circles) and calculated (open circles) parallel momentum transfer distributions for the same target-projectile combinations as in Fig. 8. The experimental data have a systematic uncertainty of 10% due to uncertainties in the beam integral and target thickness; the statistical errors of these data are small.

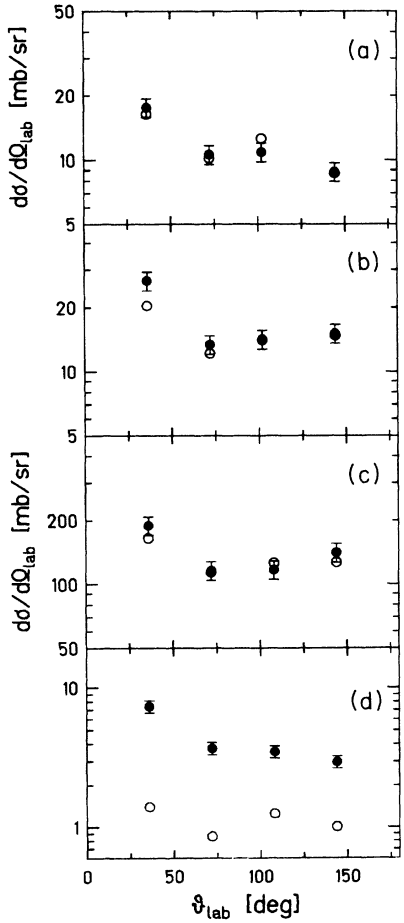

FIG. 10. Comparison between experimental (full circles) and calculated (open circles) laboratory scattering angle distributions for the same target-projectile combinations as in Fig. 8. The error bars indicate a systematic uncertainty in the beam integral and target thickness; the statistical errors of these data are small.

absolute cross sections is again apparent—the shape is reproduced well but the absolute magnitude is substantially larger than calculated. For all cases, the theoretical angular distributions were calculated on the assumption that fission occurs isotropically in the frame of the fissioning nucleus. The good agreement with experiment implies that the angular momenta of the fissioning systems are small and/or randomly oriented. The angular distributions are relatively flat showing some forward peaking caused by kinematic effects associated with momentum transfer to the fissioning system. Only for the Th data is there a slight indication of a backward enhancement. Since this is the most fissile target studied, low momentum transfer peripheral interactions will provide sufficient energy to cause fission; this is substantiated by this target having the lowest mean $p_{\parallel}$. With little forward momentum in the residual, the induced angular momentum alignment will give a $1/\sin(\theta)$ angular distribution which will be observable in the laboratory.

Figure 11 shows the comparison of calculated and experimental ΔZ distributions where the total Z of the two final fission fragments is compared to the Z of the target. Both distributions peak near the target Z but the calculations give a considerably narrower peak. This difference could be due to two effects which are difficult for us to differentiate. First, the Z distribution coming from the initial INC calculations and remaining after the fast cascade may be too narrow. There is some indication of a similar effect in the comparison of measured isotopic distributions of residues with INC calculations from the reaction Ne+Au at 8 GeV [22]. In this case the INC calculation gives a distribution which is too broad in neutron number and again a relatively sharp distribution in atomic number. The second possibility is that the angular momenta calculated for large ΔZ residuals are too low for fission to compete in the deexcitation cascade. This could be due either to the lack of collective effects in the intranuclear cascade calculation itself (which would result in too small angular momentum transfers), or to the empirical fast cascade taking away too much angular momentum. The effect of the latter is shown in Fig. 12, where calculations were performed for Nb+Au in which the particles of the fast cascade did not carry away $\frac{2}{3}$ of the maximum allowed angular momentum as in previous calculations, but only $\frac{1}{3}$ or zero. These choices increase fission for large ΔZ in better agreement with the data, but simultaneously they give much poorer agreement for $dN/dp_{\parallel}$ at large $p_{\parallel}$, and the integral cross section is also grossly overestimated. The other integral cross sections from reactions displayed in Fig. 7 also cannot be reproduced when the fast particles carry away less than our standard value of $\frac{2}{3}$ of the maximum allowed angular momentum. This may indicate that the discrepancy in

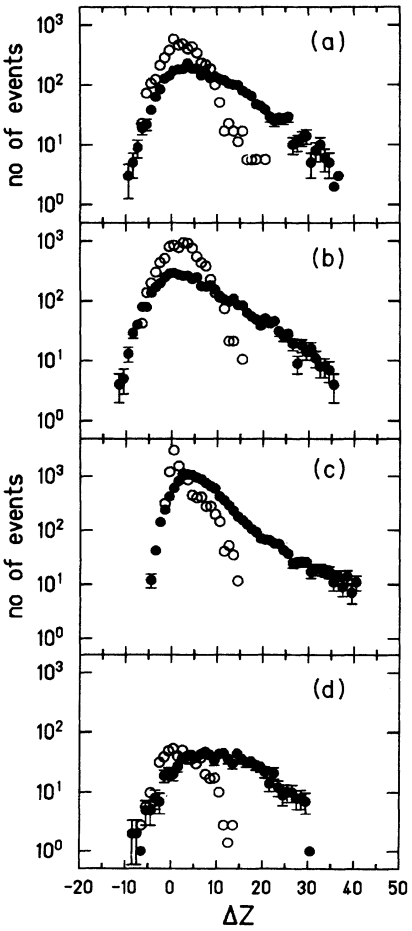

FIG. 11. Comparison between experimental (solid circles) and calculated (open circles) charge loss distributions for the same target-projectile combination as in Fig. 8. The error bars indicate the statistical errors.

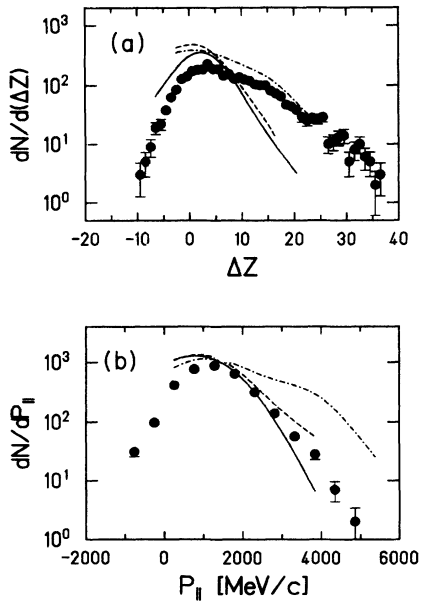

FIG. 12. (a) Effect of angular momentum removal in the fast cascade on the simulated charge loss distribution of the final reaction products in Nb+Au at 100 MeV/nucleon. The lines denote simulated distributions with different assumptions on the fraction of the maximum allowed spin that the fast particles carry away: 67% (solid line, the value used throughout this work), 33% (dashed line), and 0 (dash-dotted line). The full circles indicate the experimental results from Fig. 11. (b) Same as (a), for the parallel momentum transfer distributions. The error bars are statistical.

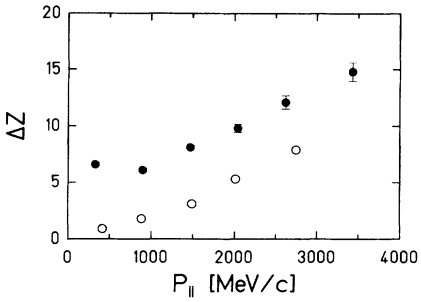

FIG. 13. Comparison between experimental (solid circles) and calculated (open circles) charge loss as a function of parallel momentum transfer for Nb+Au at 100 MeV/nucleon. The error bars show the statistical uncertainties of the mean charge losses in the respective bins of parallel momentum transfer.

the ΔZ distributions stems from an inadequacy in the calculated primary ΔZ distributions rather than in the angular momentum distributions. This interpretation is supported by the good agreement in cross sections over a wide range of target-projectile combinations and projectile energies which cover a large interval of incident angular momenta. Further evidence is shown in Fig. 13, where the experimental and calculated mean values of ΔZ as a function of $p_{\parallel}$ are compared for the same reaction. The magnitude of the disagreement is seen to be independent of momentum transfer. Since the fast cascade only affects nuclei with high linear momenta, this independence should preclude the cascade from being the cause of the discrepancy.

V. SUMMARY

We have presented an attempt at a complete model to describe the formation and subsequent decay (including fission) of target residues in a high-energy heavy ion reaction. The model utilizes an INC calculation for the early reaction stages followed by a fast cascade involving nucleon emission and ultimately deexcitation via standard statistical decay with fission using realistic angular momentum dependent barriers. Monte Carlo calculations utilizing this model are compared to fission data from 100 MeV/nucleon reactions with Fe and Nb projectiles on targets of Au, Th, Ta as well as with previous proton and ^{12}C data. Agreement in cross sections and distributions in parallel momentum transfer is very good. The data do show, however, an excess of fission events coming from systems with large Z losses from the initial target. There are indications that this discrepancy is due to a problem in estimating the initial Z distribution of the INC residues.

From our analysis we can conclude that a straightforward model utilizing known physics input at all stages does a reasonable job in reproducing important characteristics of fission data. We are able to correlate all of the cross sections from previous experiments and our data (except for the Fe+Ta reaction where fission becomes a 1% branch and is very sensitive to the detailed parameters in the model) with one single consistent set of parameters. In this model the cross section for large $p_{\parallel}$ decreases in agreement with the data without the need for the introduction of any new multifragment decay channels at high excitation energies. However, the failure to fit the width of the observed ΔZ distribution may be an important indication of emerging inadequacies of our simple model. We cannot, in any trivial way, adjust the model to fit the ΔZ distribution without introducing large overestimates of cross sections at high $p_{\parallel}$. This might be consistent with the introduction of a new high excitation energy decay channel involving intermediate mass fragments. Inclusion of such a channel would be very speculative at this point and a more detailed model would also require improvements in the treatment of all the stages of the decay. Such a project could be very informative but is beyond the scope of the current qualitative attempt to study the gross properties of these reactions.

ACKNOWLEDGMENTS

We are pleased to acknowledge many helpful discussions with A. Gavron and Y. Yariv. Work performed under the auspices of the U.S. Department of Energy by the Lawrence Livermore National Laboratory under contract No. W-7405-Eng-48 and the Los Alamos National Laboratory under Contract No. W-7405-Eng-36.

[1] V. E. Viola, Nucl. Phys. **A502**, 531c (1989).
[2] J. van der Plicht, H. C. Britt, M. M. Fowler, Z. Fraenkel, A. Gavron, J. B. Wilhelmy, F. Plasil, T. C. Awes, and G. R. Young, Phys. Rev. C **28**, 2022 (1983).
[3] A. J. Sierk, Phys. Rev. C **33**, 2039 (1986).
[4] A. Gavron *et al.*, Phys. Rev. C **35**, 579 (1987); E.-M. Eckert *et al.*, Phys. Rev. Lett. **64**, 2483 (1990).
[5] Y. Yariv and Z. Fraenkel, Phys. Rev. C **20**, 2227 (1979).
[6] Y. Yariv and Z. Fraenkel, Phys. Rev. C **24**, 488 (1981).
[7] M. Begemann-Blaich *et al.*, Phys. Rev. C **45**, 677 (1992), the preceding paper.
[8] F. Saint-Laurent, M. Conjeaud, R. Dayras, S. Harar, H. Oeschler, and C. Volant, Nucl. Phys. **A422**, 307 (1984).
[9] A. Gavron, Phys. Rev. C **21**, 230 (1980).
[10] M. M. Fowler *et al.*, Nucl. Instrum. Methods **A281**, 517 (1989).
[11] V. E. Viola and K. Kwiatkowski, Phys. Rev. C **31**, 1550 (1985).
[12] Z. Chen *et al.*, Phys. Rev. C **36**, 2297 (1987).
[13] C. M. Perey and F. G. Perey, At. Data Nucl. Data Tables **17**, 1 (1976).
[14] J. R. Huizenga and G. Igo, Nucl. Phys. **29**, 462 (1962).
[15] A. Gilbert and A. G. W. Cameron, Can. J. Phys. **43**, 1446 (1965).
[16] W. U. Schröder and J. R. Huizenga, Nucl. Phys. **A502**, 473c (1989), and references therein.
[17] J. R. Nix and W. J. Swiatecki, Nucl. Phys. **71**, 1 (1965).
[18] P. Grange, S. Hassani, H. A. Weidenmuller, A. Gavron, J.

R. Nix, and A. J. Sierk, Phys. Rev. C **34**, 209 (1986).
[19] U. Lynen *et al.*, Nucl. Phys. **A387**, 129c (1982).
[20] F. D. Becchetti, J. Janecke, P. Lister, K. Kwiatowski, H. Karwowski, and S. Zhou, Phys. Rev. C **28**, 276 (1983).
[21] A. Warwick *et al.*, Phys. Rev. C **27**, 1083 (1983).
[22] D. J. Morrisey, W. Loveland, M. de Saint Simon, and G. T. Seaborg, Phys. Rev. C **21**, 1783 (1980).